III-H Ultrafast Molecular Dynamics Studied by Time-Resolved Photoelectron Imaging

Femtosecond time-resolved photoelectron imaging is a novel experimental means to probe electronic and nuclear dynamics in real time. Since photoionization can occur from any part of the potential with any multiplicity, the method provides a universal method to follow dephasing and reaction processes.

III-H-1 Photoelectron Imaging on Time-Dependent Molecular Alignment Created by a Femtosecond Laser Pulse

TSUBOUCHI, Masaaki[1]; WHITAKER, Benjamin J.[2]; WANG, Li[3]; KOHGUCHI, Hiroshi, SUZUKI, Toshinori

([1]GUAS; [2]Univ. Leeds; [3]Dalian Inst. Chem. Phys.)

[*Phys. Rev. Lett.* **86**, 4500 (2001)]

Rotational wave packet revivals on an excited electronic state of pyrazine have been measured by femtosecond time-resolved photoelectron imaging for the first time. The pump pulse (324 nm) excited pyrazine to the S_1 0^0 level, and the subsequent 401 nm probe pulse ionized this level by a two-photon process. Figure 1(a) shows a typical photoelectron image measured at a time delay of 30 ps between the pump and probe pulses. The pump and probe laser polarization are both vertical in the figure. The observed image consists of three major rings with different radii corresponding to the photoelectron kinetic energies of 37, 101, and 643 meV. The sharp ring structure indicates that all of these ionization processes occur with the vibrational selection rule $\Delta v = 0$ via intermediate Rydberg states at the energy of $\omega_1 + \omega_2$. Strong anisotropy in the photoelectron image also points to atomic-like electron orbitals in the intermediate states. The Rydberg states contributing to the two outer rings were assigned to the 3*s* (^1A_g) and 3*p* ($^1B_{3u}$ or $^1B_{2u}$) Rydberg states. The time dependencies of photoelectron intensity for the three rings are shown in Figure 1(b). The two outer distributions decay as a function of time (τ = 110 ps), while the inner one grows with the same time constant, corresponding to the intersystem crossing from the S_1 to the triplet manifold.

We have analyzed these revival features based on the theory of RCS reported by Felker and Zewail.[1)] For simplicity, we approximated the S_1 state of pyrazine as an oblate symmetric top. By assuming the transitions from S_1 to $R_n{}^{3s}$ and to $R_n{}^{3p}$ to be parallel and perpendicular, respectively, simulation of the RCS revivals agrees almost perfectly with observation, as shown in Figure 2(b). The transition from the S_1 ($^1B_{3u}$) to the 3*p* ($^1B_{3u}$ or $^1B_{2u}$) state is vibronically induced by excitation of the mode 11 (b_{3u}), making the transition a perpendicular type.

The PAD measured at each time delay was fit to the following form:

$I(\theta) = \beta_{00}Y_{00}(\theta) + \beta_{20}Y_{20}(\theta) + \beta_{40}Y_{40}(\theta) + \beta_{60}Y_{60}(\theta)$,

where Y_{LM} are spherical harmonics. We found β_{60} to be negligible. The ratio β_{20}/β_{00} thus obtained for ionization of S_1 via the 3*s* and 3*p* Rydberg states also clearly shows the rotational revivals [Figure 1(c)]. In the present case, the pump pulse creates a time-dependent alignment $A_{20}(t)$ in the S_1 state, and the probe pulse transfers this alignment to rotational levels in the Rydberg states. Since these states are ionized instantaneously within a probe laser pulse, the PAD is modulated only by the time dependence of $A_{20}(t)$ in the S_1 state.

Reference

1) P. M. Felker, J. S. Baskin and A. H. Zewail, *J. Phys. Chem.* **90**, 724 (1986).

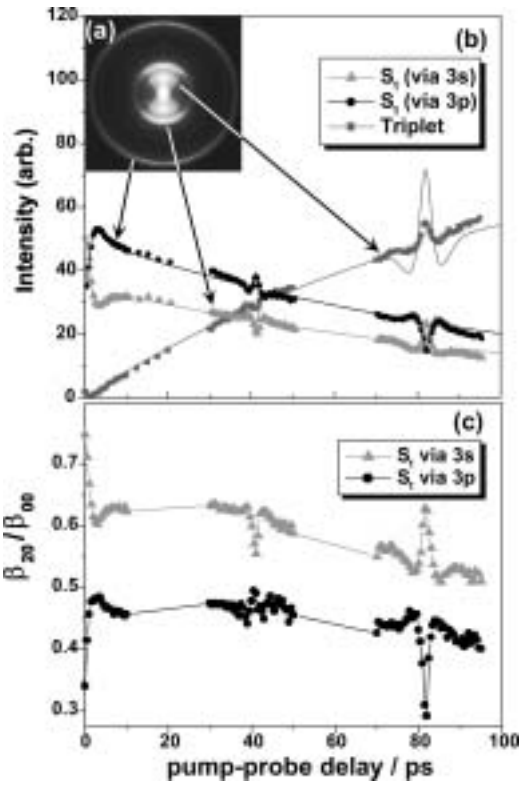

Figure 1. (a) Inverse Abel transformed photoelectron image of the [1+2'] PEI of pyrazine via the S_1 $B_{3u}(n\pi^*)$ 0^0 level observed at the time delay of 30 ps. The original image was integrated 80 000 laser shots. (b) Time evolution of three major components in the [1+2'] PEI. Circle (●), triangle (▲), and square (■) represent the angle integrated intensity for the outer (KE = 643 meV), middle (101 meV), and inner ring (37 meV), respectively. Solid lines are a simulation taking into account the rotational coherence. (c) β_{20}/β_{00} as a function of pump-probe time delay in the [1+2'] PEI.

III-H-2 Femtosecond Photoelectron Imaging on Pyrazine: Spectroscopy of 3*s* and 3*p* Rydberg States

SONG, Jae Kyu[1]; TSUBOUCHI, Masaaki[2]; SUZUKI, Toshinori
([1]Seoul Natl. Univ.; [2]GUAS)

[*J. Chem. Phys.* **115**, 8810 (2001)]

Femtosecond two-color and one-color photoelectron imaging have been applied to Rydberg states (n = 3) of jet-cooled Pyrazine. The 3s and 3p members of Rydberg series converging to the ground state (n^{-1}) of the cation and the 3s member of Rydberg series converging to an excited state of the cation (π^{-1}) were observed. Figure 1 (a) shows (2+1) REMPI spectrum of jet-cooled Pyrazine observed with our tunable femtosecond laser. There are two band systems. The first system exhibits a progression of the 6a mode, indicating the geometry change from S_0 along this mode. The second system does not indicate such a prominent geometry change. Figure 1 (b) is the He(I) photoelectron spectrum of Pyrazine adopted from the literature.[1)] Here, the first system is the ground state (^2A_g) of the cation and the second system is the excited state ($^2B_{1g}$) of the cation. The spectral features in Figure 1 (a) and (b) are remarkably similar, from which the two systems in Figure 1 (a) are assigned to 3(n^{-1}) and 3s(π^{-1}) Rydberg states. The energy difference between the 3s(π^{-1}) and 3s(n^{-1}) Rydberg states is 820 meV, while the energy difference between $I_0(^2A_g)$ and $I_1(^2B_{1g})$ is 880 meV. The quantum defects calculated for the 3s(π^{-1}) and 3s(n^{-1}) Rydberg states are 0.87 and 0.86, respectively. The difference in electronic character between the 3s(π^{-1}) and the 3s(n^{-1}) Rydberg states was also evident in the photoelectron angular distributions for ionization out of these orbitals.

The spectrum shown in Figure 1(b) is strikingly different from the one reported by Turner *et al.* using a nanosecond laser[2)] in that (1+2) REMPI spectrum via T_1 is completely missing in our data. This is presumably because the ionization efficiency of the rapidly-decaying Rydberg states was substantially lower with nanosecond lasers, making the $T_1 \leftarrow S_0$ spectrum more dominant.

The Franck-Condon factors in electronic transitions involving S_0, S_1, S_2, 3s(n^{-1}), 3s(π^{-1}), D_0, and D_1 were analyzed to examine conical intersections between these states, and the intersection was identified between S_1-S_2, 3s(n^{-1})-3s(π^{-1}) and D_0-D_1. Although the electronic dephasing times for S_2-S_1 and D_1-D_0 have been estimated to be 30 fs, the photoelectron angular distribution indicated that 3s(n^{-1})-3s(π^{-1}) dephasing is not completed within 100 fs.

References

1) H. Fridh, L. Asbrink, B. O. Jonsson and E. Linddholm, *Int. J. Mass Spectrom.* **8**, 101 (1972).
2) R. E. Turner, V. Vaida, C. A. Molini, J. O. Berg and D. H. Parker, *Chem. Phys.* **28**, 47 (1978).

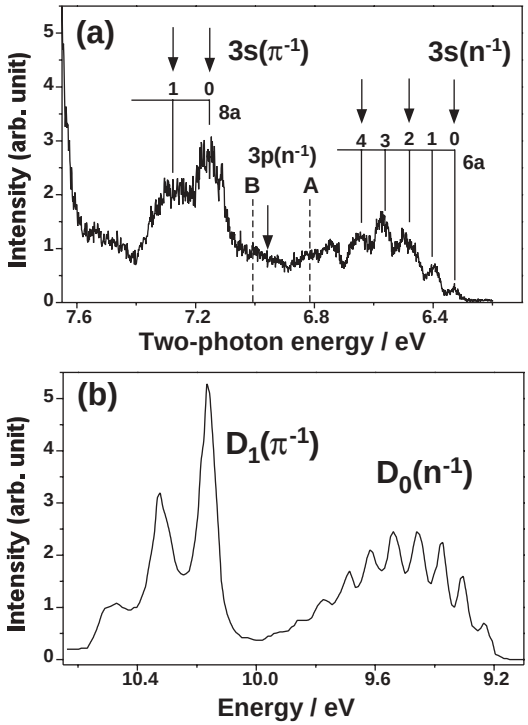

Figure 1. (a) One-color REMPI spectrum in the 325–400 wavelength region. The abscissa of the spectrum represents the two-photon energy in eV. The assignments of the vibrational progressions are indicated in the figure. The origins of 3pA and 3pB Rydberg states, although they are not visible in the spectrum, are indicated by broken lines. (b) He (I) photoelectron spectrum of Pyrazine shown on the same scale as (a). Adopted from reference 1.

III-H-3 Photoionization Dynamics of CO Studied by Photoelectron Imaging

KATAYANAGI, Hideki; MATSUMOTO, Yoshiteru; DE LANGE, Cornelis A.; SUZUKI, Toshinori

The photoelectron energy and angular distributions in (2+1) REMPI of CO via the $B^1\Sigma^+$ (v' = 0 and 1) states have been observed by photoelectron imaging. Jet-cooled CO molecule was ionized using UV light near 230 nm, and the photoelectrons were projected onto a position-sensitive imaging detector.

Since the $B^1\Sigma^+$ (v' = 0) state is the 3s member of a Rydberg series converging to the $X^2\Sigma^+$ (v^+) state of CO^+, the Δv = 0 propensity rule may be anticipated. However, off-diagonal transitions, Δv = 1–7, were observed. Figure 1 shows the observed photoelectron image. Two outer rings with strong intensity arise from Δv = 0 and 1 transitions corresponding to the photoelectron kinetic energy of 2.15 and 1.88 eV, respectively. In addition, close examination reveals that there are weak inner rings due to Δv = 2–7 transitions. The rings were separated by about 260 meV in energy. These results are in agreement with a previous work by Sha *et al.*[1)] The photoelectron angular distribution exhibited high anisotropy for v^+ = 0 and a low value for v^+ = 1–7, which suggests different ionization mechanisms between the Δv = 0 and Δv = 1–7 ionization processes. The latter, off-diagonal transitions, are

ascribed to autoionization from a superexcited Rydberg state converging to the first excited ionic state ($A^2\prod$).

In the photoelectron spectrum via $B^1\Sigma^+$ (v' = 1) state, the Δv = 0 transition was dominant, which is different from the spectrum via $B^1\Sigma^+$ (v'= 0).

References

1) G. Sha, D. Proch, Ch. Rose and K. L. Kompa, *J. Chem. Phys.* **99**, 4334 (1993).

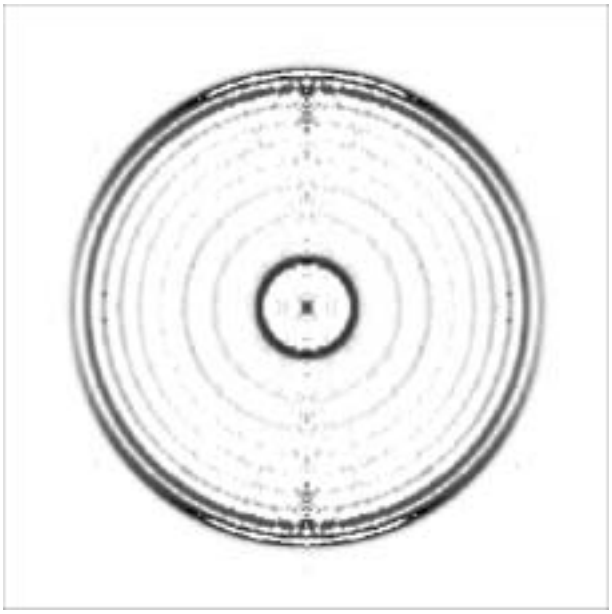

Figure 1. Inverse Abel transformed (512 × 512 pixels) photoelectron image of [2+1] REMPI of CO via the $B^1\Sigma^+$ (v' = 0) state. The original image was integrated for 90,000 laser shots.

III-I Bimolecular Reaction Dynamics

Chemical reactions under thermal conditions occur with various collision energies, internal quantum states, and impact parameters. The experimental data measured under such conditions are highly-averaged quantities, from which detailed feature of reactions can hardly be learned. A crossed molecular beam method allows us to observe chemical reactions of state-selected reagents at well-defined collision energy. The differential cross section (angular distribution of products) reveals impact-parameter dependence of reaction probability and reaction mechanism.

III-I-1 Differential Cross Sections for the Inelastic Scattering of NO ($X^2\prod_\Omega$) by Ar Studied by Crossed Molecular Beam Ion-Imaging and Quantum Scattering Calculations

KOHGUCHI, Hiroshi; SUZUKI, Toshinori; ALEXANDER, H. Millard[1]
([1]Univ. Maryland)

[*Science* **294**, 832 (2001)]

High-resolution ion-imaging combined with a crossed molecular beam method has been applied to the state-resolved differential cross sections (SR-DCSs) of inelastic scattering of NO (j" = 0.5, Ω" = 1/2) + Ar → NO (j', Ω' = 1/2, 3/2) + Ar at a collision energy of 516 cm^{-1}. Sensitive (j', Ω')-dependence and complex undulations of the obtained SR-DCS were investigated by comparison with rigorous theoretical calculations. The close-coupling scattering calculation without any dynamical approximation based on the two ab initio potential energy surfaces [CEPA and CCSD(T) calculations] were carried out for the theoretical SR-DCS. The above quantum features observed in the ΔΩ = 0 scattering were almost completely reproduced by the two *ab initio* surfaces consistently. Noticeable discrepancy between the two calculations, although the CCSD(T) potential energy surfaces yielded the better agreement with the experiment, was seen in the forward scattering of the middle Δj in the ΔΩ = 1 transitions. The major difference between the CCSD(T) and CEPA surfaces lying in the potential well region at the T-shaped configuration resulted in these discrepancies of the specific scattering angles in the limited (j', Ω') states.

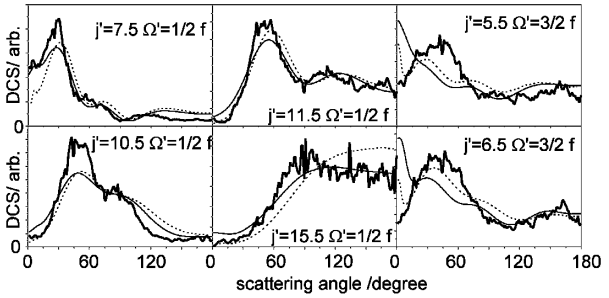

Figure 1. State-resolved differential cross sections of the NO + Ar inelastic scattering at the collision energy of 516 cm^{-1}. The initial state of the collision is j" = 0.5, Ω" = 1/2 state. The thick-solid lines represent the experimental differential cross sections. The thin-solid and broken lines are the theoretical results based on the CCSD(T) and the CEPA *ab initio* PESs, respectively.